Composites Science and Technology 211 (2021) 108864

Contents lists available at ScienceDirect

Composites Science and Technology

journal homepage: www.elsevier.com/locate/compscitech

Controlling glass bead surface functionality - Impact on network formation in natural edible polymer systems

Silvia Brandner [a], Tim Kratky [b], Kerstin Holtz [a], Thomas Becker [a], Mario Jekle [a,*]

[a] Technical University of Munich, Institute of Brewing and Beverage Technology, Research Group Cereal Technology and Process Engineering, 85354, Freising, Germany
[b] Technical University of Munich, Catalysis Research Center, 85748, Garching, Germany

ARTICLE INFO

Keywords:
Particle-reinforced composites
Coupling agents
Interfacial strength
Photoelectron spectroscopy

ABSTRACT

Combining particles and polymers provides materials with unique mechanical properties. Hereby, the character of the particle surface is important for the network properties. However, particle-polymer interfaces of food systems are scarcely controllable. This often leads to an indefinite contribution on the network properties. Developing hybrid artificial systems by using inert particles with a well-defined coating represents a new approach in food science. Coating with functionalized silanes enables the imitation of naturally occurring chemical groups. A novel experimental approach involving nano- and macroscopic analytical techniques (X-ray photoelectron spectroscopy and contact angle) sheds light on the nature and the strength of the adsorption. Depending on the presented surface functionality, strong specific to weak unspecific adsorptions arise, e.g. amino-functionalized surfaces show strong interaction with protein, while almost no interaction was observed with an aliphatic surface. Based on these different particle adhesivenesses, the monitoring of network formation discloses a significant impact of particle surface functionality on network development of food matrixes. An increasing network development time (3.2–6.0 min, gluten protein-based) in combination with a decreasing network strength (874-464 mNm gluten protein-based) correlates with an increasing adhesiveness of particles. Thus, using functionalized particles clearly demonstrates the importance of particle surface functionality on network properties in food systems.

1. Introduction

Polymer systems, filled with small particles like carbon black or silica, are widely used in material sciences and applications to improve the mechanical properties by increasing tensile strength or elongation at break [1,2]. These enhanced material properties are mediated by physical and chemical interactions between particle surface and polymer matrix. Beside these designed systems, highly complex particle-polymer systems occur also naturally in foods. Particle-polymer based foods are present at different processing steps: in a non-processed form as raw materials, like wheat kernels, in a processed form, like cheese, dough, sausages, or in a highly processed manner as designed foods for specific applications, like nutraceuticals. For most particle-polymer based food systems, the polymeric matrix consists of proteins or carbohydrates [3], whereas the particles could be of very different character, especially regarding the rigidity. In wheat kernels or dough, rigid starch particles are embedded in gluten-based protein matrices, whereas in cheese or sausages soft oil particles are embedded in protein matrices. Despite this difference in particle rigidity, foods containing soft oil droplets are also considered as particle-filled composite materials. In general, all these systems have in common, that the analysis of the particle-polymer interface is challenging. In the following, the difficulties in analyzing particle-polymer interfaces of complex food systems supplemented with rigid particles are discussed, using the example of wheat dough, a very frequently processed food pre-product: From a general point of view, particles affect polymer networks mainly by three factors: the particle shape, the size/size distribution and the surface functionality [2,4–6]. Independent of shape and size, surface functionality can be regarded as universal factor, because the surface contributes to the interface between particle and polymer. Therefore, it defines the kind of possible interactions [7]. To analyze the impact of this interface on the network formation, different approaches are used in food science. The most common methods are reconstitution experiments [8] or the modification of a particle (starch) surface by mechanical/chemical treatment [9–11]. However, these methods have several disadvantages. Reconstitution experiments, in

* Corresponding author.
E-mail address: mjekle@tum.de (M. Jekle).

https://doi.org/10.1016/j.compscitech.2021.108864
Received 12 March 2021; Received in revised form 5 May 2021; Accepted 12 May 2021
Available online 16 May 2021

which polymeric wheat proteins (gluten) and particulate starch (~1–80 μm) of different origin and nature are mixed in quantities that correspond to wheat flour, modify not only the surface functionality [12] but also the shape and size of starch. In addition, exchanging the starch origin and quality causes different compositions of surface-active proteins and lipids [10,13]. Therefore, the impact of a specific functional group, in mediating a specific interaction, like hydrogen bonds or hydrophobic interactions, can not be identified. Consequently, reconstitution experiments only contribute to the general importance of particle (starch) properties to the overall (food) system, but do not clarify the influence of surface functionality [14]. In addition, modification of a particle (starch) surface by removing lipids or proteins does not offer a clear assignment of surface functionality on the material properties. The required aggressive chemicals or high temperatures often cause additional modifications of particles (starch) regarding their porosity or agglomeration properties [15]. In summary, the common approaches only reveal the importance of the particle (starch) functionality on the network properties in a rather general manner without delivering any mechanistic relations. These above described problems are highly relevant as they occur in every natural particle-polymer based food system. Therefore, approaches, which enable a target manipulation restricted to the particle surface only, are indispensable for clarifying the impact of the particle surface on the network formation and behaviour in food-based systems. A promising approach relies on the replacement of natural particles by inert artificial microspheres of comparable size and shape. They offer the advantage of a controllable surface functionality [16–18]. In the field of food science, a few studies are available, where natural particles were replaced by artificial particles with modified surface properties based on coatings. Coating surfaces with whole proteins or fats leads to adsorbed structures in an undefined way [16,17]. In contrast, using coupling agents like silanes or cross-linkers, enable the creation of well-defined, homogeneous and stable surfaces bearing just a single functionality. The high amount of commercially available silanes and a well-established synthetic pathway allow for the imitation of nearly every natural occurring functional group of food-based particles. In this study, four different silanes and two heterobifunctional cross-linkers are used to imitate common functional groups of food particle surfaces and their impact on network formation in protein- or carbohydrate-based matrixes. For the imitation of the hydrophobic and non-polar character of fats (alkyl chains), a propyl-functionalized silane is used. Hydrophilic and polar/ionic parts are imitated by a silane bearing cyano groups, sulphur-containing parts by a mercapto-functionalized silane and nitrogen-containing parts by an amino-functionalized silane. In addition, two different heterobifunctional cross-linkers were used to reproduce the possibility of polymers to covalently bind to a particle surface and to enhance the effects arising from a covalent interaction between functionalized surface and polymer. In the following, functionalized surfaces are prepared, validated and analyzed, regarding their interface characteristics, with two common food polymers (protein- and carbohydrate-based). A systematical approach of using varying rinsing steps enables the analysis of adsorption and desorption kinetics on a nano- and macroscopic level within a model system. Based on the revealed adsorption mechanisms and adhesiveness between imitated functional group and polymer, the impact of particle surface functionality and network formation is discussed.

2. Experimental

2.1. Materials

Glass beads, with a size ranging from 2.60 μm to 19.27 μm, which is comparable to that of microscopic food particles, were purchased from Microperl Sovitec (Schönborn, Germany). Glass plates (microscope slides) were purchased from VWR (Darmstadt, Germany) and silicon wafers were purchased from Wacker Chemie (Munich, Germany). Silane coupling agents - 3-aminopropyltriethoxysilane (amino-silane, 98%), 3-mercaptopropyltriethoxysilane (mercapto-silane, 98%), *n*-propyltriethoxysilane (propyl-silane, 97%), 2-cyanoethyltriethoxysilane (cyano-silane, 97%) - were purchased from ThermoFisher (Germering, Germany) and Alfa Aesar (Karlsruhe, Germany). For the covalent attachment of mercapto-coated surfaces with the polymeric matrix, two heterobifunctional cross-linkers were purchased from Sigma Aldrich (Taufkirchen, Germany): *N*-succinimidyl 3-maleimidobenzoate (MBS) for the coupling with the protein-based (gluten) polymer matrix and *N*-[p-maleimidophenyl] isocyanate (PMPI) for the coupling of the carbohydrate-based (hydroxypropylcellulose) polymer matrix. For the protein-based food matrix vital gluten (Kröner-Stärke, Ibbenbüren Germany) was used. For the carbohydrate-based food matrix with similar mechanical properties as gluten [18], hydroxypropylcellulose HPC (Klucel H, Kremer Pigmente, Aichstetten Germany) as major component (4:1 parts) and polyvinylpyrrolidone (PVP K 90, VWR, Darmstadt, Germany) were used.

2.2. Sample cleaning

Glass beads/plates were cleaned by submergence in a freshly prepared piranha solution, consisting of 1.5 parts H_2O_2 (30%) and 3.5 parts H_2SO_4 (98%) at 95 °C under gentle stirring for 30 min. After a sedimentation time of 120 min, the glass beads were rinsed using ten centrifugations (1500xG for 5 min), replacing the supernatant with distilled water between the steps. Afterwards, a neutral pH value of the supernatant indicated the adequate replacement of piranha solution. Glass beads were stored in distilled water. Glass plates were directly removed from the piranha solution and rinsed with distilled water two times for 5 min each. Si wafer were prepared for coating by annealing at 900 °C for 1 h in air.

2.3. Surface functionalization

For coating of the surfaces, 1% (v/v) of silane was hydrolyzed in a 95/5 (v/v) mixture of ethanol/distilled water, adjusted to a pH value of 4.5 by adding hydrochloric acid and stored for 12 h at room temperature. Silylation was carried out at 70 °C for 30 min under gentle stirring. For glass beads, the supernatant was decanted, prior to silylation. After silylation, glass beads were rinsed using four centrifugations (25xG for 6 min), with a replacement of the supernatant with fresh ethanol/distilled water (95/5 v/v) in between the steps to remove unreacted silane. Glass plates were rinsed two times for 5 min each in ethanol/distilled water (95/5, v/v). All samples were dried at 120 °C for >1 h. Functionalized SiO_2 surfaces were rinsed after drying three times for 5 min in ethanol/distilled water (95/5 v/v).

2.4. Attachment of heterobifunctional cross-linkers

The heterobifunctional cross-linker, MBS or PMPI, was attached to mercapto silane-coated samples. Prior to crosslinking, glass beads were soaked in distilled water for 15 min. Subsequently, excess water was removed by centrifugation (15 min at 1000xG). Functionalized Si wafers were directly used. MBS was diluted to a final concentration of 75 mM for glass beads or ~0.02 mM for Si wafers in a 1:1 mixture of DMSO and phosphate buffered saline (PBS). PMPI was diluted to a final concentration of 50 mM for glass beads and ~0.02 mM for SiO_2-surfaces in DMSO, respectively. After 1 h of incubation, excess cross-linker was removed by rinsing in the pure solvent. For glass beads rinsing was applied by three centrifugations at 1500xG for 3 min. Between the centrifugations, the supernatant was replaced by PBS for MBS or by DMSO for PMPI. Thereafter, glass beads or functionalized Si wafers were directly used.

2.5. Interactions of polymers with functionalized SiO_2 surfaces

To assess the adhesiveness of the silane coatings towards the protein or carbohydrate-based matrix, the functionalized Si wafer were incubated in gliadin/EtOH solution (300 mg/L in 60/40 EtOH/H2O dest.) or HPC-PVP/dest. H_2O solution (1% polymers v/v, with 1 part PVP and 4 parts HPC) at room temperature for 30 min under gentle stirring. Since not the whole gluten polymer is soluble, the ethanol soluble gliadin fraction was used in order to prove the adsorption properties between the wafer and the gluten polymer. After incubation, the adhesiveness between polymer und wafer was analyzed by applying different rinsing intensities (none; 1 min, 5 min, 30 min) in the corresponding solvent of the used polymer. Before analysis, the samples were dried at 60 °C for 1 h.

2.5.1. Contact angle measurements

The functionalized Si wafers (see 2.3–2.5) were analyzed by sessile drop method using a drop shape analyzer (DSA25 Krüss, Germany).

2.5.2. X-ray photoelectron spectroscopy (XPS)

X-ray photoelectron spectra were recorded on a Leybold-Heraeus LHS 10 spectrometer using a non-monochromatized Mg Kα source (1253.6 eV). All coated glass beads, except propyl, were pressed into cavities and measured as pellets. Functionalized Si wafers were directly mounted on a sample holder. For the detection of the propyl coating on a glass surface, a coated and a reference glass piece were mounted on a sample holder and annealed at 150 °C overnight before measurement. All spectra were recorded in an ultra-high vacuum chamber at a pressure below 5×10^{-8} mbar. The analyzer was operated at a constant pass energy of 100 eV leading to an energy resolution with a full width at half-maximum (fwhm) of ~1.1 eV. The energy scale of the spectra was corrected for sample charging by using the Si 2p signal at 103.3 eV (SiO_2). Core level spectra were deconvoluted by using Voigt functions after linear background subtraction.

2.6. Interactions of polymers with functionalized glass bead surfaces

2.6.1. Fluorescence labeling

Based on the ability of amino and mercapto groups to interact with fluorescein-5-isothiocyanat or *N*-(5-fluoresceinyl)maleimide, respectively, the coverage of the glass bead surface by amino or mercapto silanes can be analyzed by confocal laser scanning microscopy (CLSM). For dye labelling, approximately 0.5–1.0 g of coated and uncoated (reference) glass beads were stirred in ethanol with 0.01 g dye per 10 ml for 15 min at room temperature. For amino silane fluorescein-5-isothiocyanat (Merck, Germany) and for mercapto silane *N*-(5-fluoresceinyl)maleimide (Sigma Aldrich, Germany) was used. Labeled samples were washed by centrifugation (6 times at 25 x G for 3 min) with ethanol until the supernatant became colorless. Labeled and washed glass beads were placed onto a hemocytometer, which was used as object carrier. For visualization, an eclipse Ti–U inverted microscope with an e-C1 plus confocal system (Nikon GmbH, Düsseldorf, Germany), a Plan Apo VC 60x/1.40 oil objective and 534 nm and 488 nm lasers was used. Three images of the coated and uncoated glass particles, each with a resolution of 1024 × 1024 pixel (size 215 × 215 μm) and at a different position in z-direction, were acquired.

2.6.2. Network formation of food matrices

For analyzing the effect of the particle-polymer interface on the network formation in complex food matrices, different polymer-particle systems were hydrated and mixed (gluten or HPC/PVP-based) by using a recording z-kneading system (DoughLAB, Perten Instruments, Hamburg, Germany). For monitoring the network formation, all systems were mixed for 20 min at a speed of 63 rpm at 30 °C. To produce optimal developed (max. mNm) polymer particle systems, protein-based matrixes were mixed for 7 min and carbohydrate-based systems 8 min.

Table 1
Food matrix composition and particle proportion. Quantity in parts.

Matrix type	Distilled water	Glass beads	Gluten	HPC	PVP
Protein	1	1.59	0.68	/	/
Carbohydrate	1	0.74	/	0.25	0.07

Table 1 shows the used amounts of polymers and glass beads for the different systems. The amount of water and polymer used is based on a previous study [18].

3. Results and discussion

3.1. Polymer adsorption on functionalized surfaces

The characteristics of the interface between differently functionalized surfaces and two common food matrixes (protein- and carbohydrate-based) are analyzed regarding their adsorption and desorption kinetics (adhesiveness) on a nano- and macroscopic level. Since coating and characterization of an ideally flat and well-defined surface is simplified compared to a heterogeneous spherical surface (particles), SiO_2 surfaces serve as a model system for glass beads. After annealing in air, the atomically flat and single-crystalline surface of a Si wafer is oxidized to SiO_2 and, hence, chemically identical to quartz glass. Therefore, results obtained from this model system are highly comparable to those of functionalized glass beads. In total, 10 different systems were analyzed: Propyl-, cyano-, amino- and mercapto-functionalized SiO_2 surfaces in combination with HPC-PVP and gliadin, respectively, MBS-functionalized SiO_2 surfaces in combination with gliadin, and PMPI-functionalized SiO_2 surfaces in combination with HPC-PVP. Thereby, the protein-based matrix is represented by gliadin and the carbohydrate-based by HPC-PVP. Contact angle measurements monitor surface characteristics at the macroscale, based on the hydrophobicity of the surface. Therefore, modified wetting properties of water droplets are capable to detect functional groups and even adsorbates. In contrast, XPS is a surface-sensitive method, which characterises the chemical composition on the nanoscale. A successful functionalization of the SiO_2 surfaces was confirmed by XPS and contact angle measurements for all systems. Specific core levels of the functional groups were detected in XPS: C 1s peak for propyl groups (285.2 eV), N 1s peak for cyano and amino groups as well as for the PMPI and MBS cross-linkers (400.0, 399.7, 401.0 and 401.3 eV, respectively) and S 2s peak for mercapto groups (227.3 eV) [25]. In addition, the functionalized SiO_2 surfaces show various contact angles between water droplets and surface, depending on the hydrophobic/hydrophilic character of the coating (compare Fig. 2 a). For the propyl coating, a contact angle of 99.2 ± 1.5° demonstrates the hydrophobic character. In contrast, mercapto (69.7 ± 5.7°) and cyano (64.9 ± 0.8°) coatings show a lower hydrophobicity due to their lower contact angles. The amino functionalization induces nearly full wetting (29.6 ± 8.8°) due to a strong hydrophilic character. Attaching cross-linkers to the mercapto coating, causes further modifications of the surface; PMPI slightly increases (71.1 ± 2.2°), whereas MBS reduces the hydrophobic character (65.8 ± 1.7°). The experimental approach for the assessment of polymer adhesiveness on differently functionalized SiO_2 surfaces is summarized in Fig. 1. By comparing contact angle and XPS data of the functionalized SiO_2 surfaces before (reference) and after incubation in a polymer solution, the adsorption of the polymers can be analyzed. The subsequent rinsing steps of different durations assess the desorption and, thus, determine the adhesiveness between polymer and functionalized surface.

After incubation in a carbohydrate-based (HPC-PVP) or a protein-based (gliadin) polymer solution, the surface is completely covered by the polymer, independent of the coating. Therefore, contact angles are in a small range between 31.8 ± 3.7° for HPC-PVP and 30.8 ± 6.7° for gliadin for every coating. The low standard deviations of 3.4 and 6.7°,

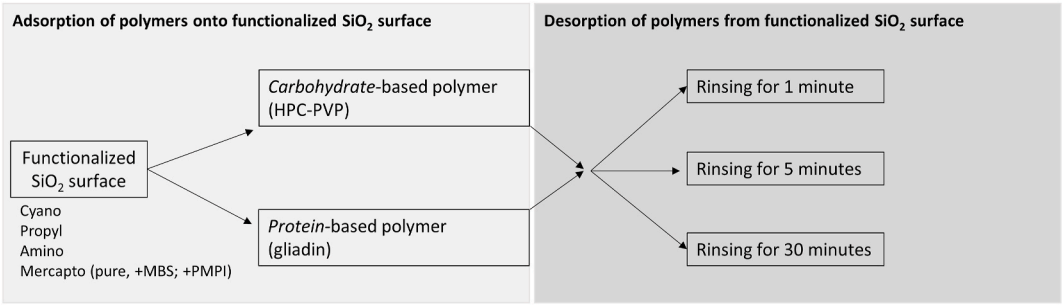

Fig. 1. Experimental approach for analyzing the adsorption and desorption properties of polymers towards differently functionalized surfaces (cyano-, propyl-, amino-, mercapto-, MBS-, PMPI-coated). Contact angle and XPS were measured after each step.

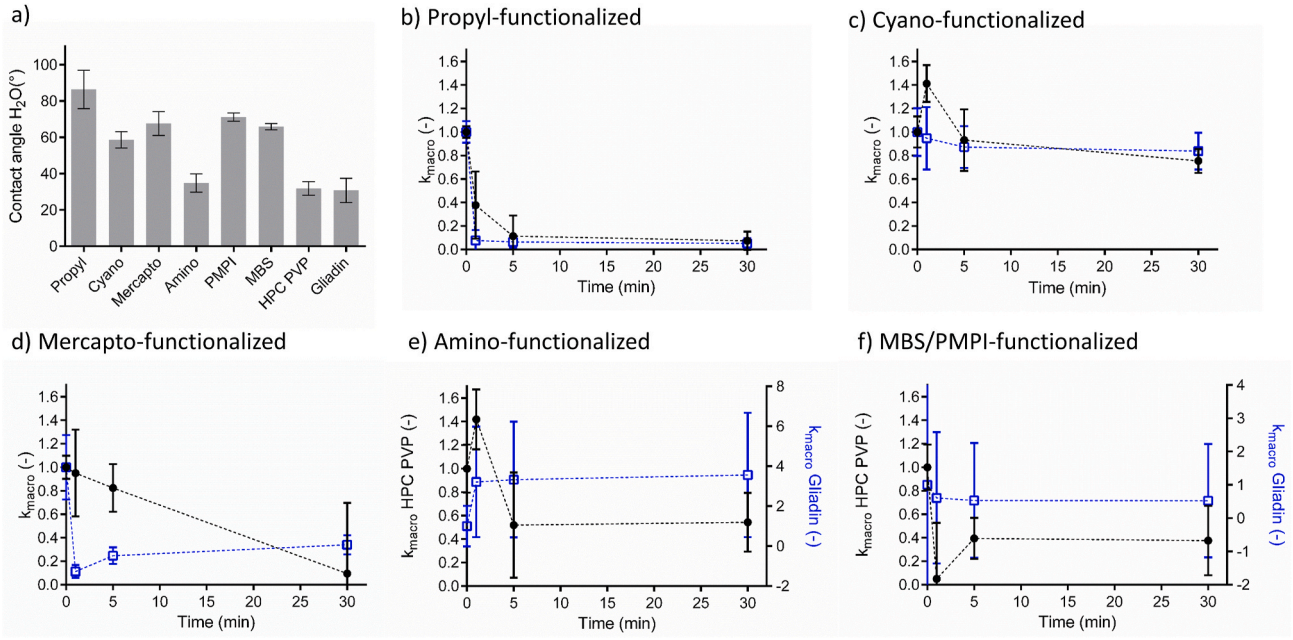

Fig. 2. Evaluation of polymer adhesiveness on functionalized SiO_2 surfaces by contact angle measurements. Coating and incubation in polymer solution in a). Adhesiveness, expressed by k_{macro}, over rinsing time of HPC-PVP (●) and gliadin (□) in b) - f) depending on surface functionalization: propyl-functionalized surface in b), cyano-functionalized surface in c), mercapto-functionalized surface in d), amino-functionalized surface in e) as well as MBS- (for gliadin) and PMPI (for HPC-PVP)-functionalized surface in f). For better visualization in e) and f), gliadin is plotted versus a separate y-axis (right side). Means are shown with standard deviation (a) or propagation of error considering the standard deviation (b–f).

respectively indicate the formation of a homogenous polymer layer which covers the surface entirely. XPS confirms these results as the Si 2p peak originating from the SiO_2 surface is almost completely attenuated by a covering adlayer.

3.2. Evaluation of polymer desorption from functionalized surfaces

For the assessment of the polymer adhesiveness, the rinsing induced desorption of the polymers from the functionalized SiO_2 surfaces is evaluated. Due to different functional groups present in the coating, neither absolute values for the contact angle, nor absolute XPS intensities of a single surface, provide reasonable numbers to address the desorption behavior. Hence, we defined macro- and nanoscopic coefficients to evaluate the polymer adhesiveness as a function of the rinsing time by comparing the functionalized surface before and after polymer incubation with the rinsed surfaces. The results and discussion of contact angle and XPS data for every coating and polymer can be found in the supplementary data. The surface modification observed by contact angle measurements, is assessed by the macroscopic adsorption coefficient k_{macro}, which is defined as follows:

$$k_{macro} = \left|\frac{\alpha_{coating} - \alpha(t)}{\alpha_{coating} - \alpha_0}\right| \quad (1)$$

$\alpha_{coating}$ corresponds to the contact angle measured on a functionalized SiO_2 surface, α_0 to the contact angle directly after polymer incubation and α(t) to the contact angle after a certain rinsing time. Based on the amount of adsorbed/desorbed polymers on the functionalized surface over rinsing time, the contact angle varies. If α(t) is equal to $\alpha_{coating}$, no polymer is adsorbed anymore and $k_{macro} = 0$. In contrast, if α(t) is equal to α_0, all polymers remain adsorbed at the surface and $k_{macro} = 1$. The error of k_{macro} was calculated based on the propagation of error considering the standard deviation of the respective contact angles.

k_{nano} was calculated based on XPS data. Characteristic core levels for the coating as well as the polymers were identified. In most cases, distinct components of the C 1s core level could be attributed to either the polymer or the coating. Deconvolution of the signals (see supplementary information) reveals the peak area of each component ($A_{polymer}$ and $A_{coating}$). We defined k_{nano} to reflect the amount of polymers adsorbed on the functionalized SiO_2 surface as a function of the rinsing time t as follows:

$$k_{nano} = \frac{A_{polymer}(t)}{A_{coating}(t) + A_{polymer}(t)} \cdot \frac{A^0_{coating} + A^0_{polymer}}{A^0_{polymer}} \quad (2)$$

The second term scales k_{nano} with respect to the initial peak ratio obtained directly after incubation with the polymer and, hence, offers values for k_{nano} that are comparable to k_{macro}.

3.2.1. Carbohydrate-base polymer desorption

Depending on the surface functionalization, the consideration of k_{macro} for HPC-PVP incubated surfaces (Fig. 2 b-f), demonstrates different desorption behaviors. A propyl-functionalization already causes a significant decrease of k_{macro} after 1 min of rinsing. k_{macro} stabilizes at a diminutive value of 0.11 ± 0.18 after 5 min. In contrast, k_{macro} of the amino-, cyano- and PMPI-functionalized systems decreases immediately but stabilizes at significantly higher values after 5 min of rinsing; k_{macro} of the amino-functionalization corresponds to 0.52 ± 0.44, the cyano-functionalization to 0.93 ± 0.26 and the PMPI-functionalization to 0.39 ± 0.17. Interestingly, a mercapto-functionalization results in a constant decrease of k_{macro} over the entire rinsing time to a final value of 0.10 ± 0.60. The fast and tremendous decrease of $k_{macro,\ propyl}$ evidences a negligible adhesiveness of HPC-PVP to the hydrophobic coating. Since HPC, respectively PVP, are hydrocolloids, their low affinity to a hydrophobic surface is reasonable. The stabilization of k_{macro} at higher values proves a higher adhesiveness to other coatings. Based on the equilibrium value of k_{macro}, the functionalized surfaces can be ranked with respect to the adhesiveness of HPC-PVP: cyano > amino > PMPI. Note that k_{macro} for amino- and cyano-functionalized surfaces is larger than 1 after the 1 min of rinsing (Fig. 2 c & e). According to its definition, $k_{macro}>1$ might correspond to an increase of polymer adsorbed to the surface, which is excluded in our experimental setting. Considering the high water solubility of the hydrocolloids, it is reasonable that excess quantities present after incubation will dissolve in the water droplet during contact angle measurement. As the properties of the probing water droplet are now changed this might force a spreading of the water droplet resulting in lower contact angles and consequently in values of $k_{macro}>1$. After a first rinsing, the weakly bound fraction of polymer has been desorbed and, thus, k_{macro} becomes <1. The persisting decrease of $k_{macro,\ mercapto}$ is rather unexpected. However, the standard derivations indicate a highly inhomogeneous surface and thus, a desorption behavior which cannot be determined unambiguously based on the macroscopic approach. k_{nano} essentially confirms the observations of k_{macro} (compare Fig. 2 b-f) with Fig. 3 a-e)) and also gives rise to a ranking of the polymer adhesiveness: amino > PMPI > propyl. Compared to the macroscopic approach, the detection limit for adsorbates is higher in XPS. Therefore, $k_{nano,\ propyl}$ is higher than $k_{macro,\ propyl}$ during all rinsing steps. The substantial decrease of $k_{macro,\ propyl}$ demonstrates that the small amount of polymer remaining on the coated surface is still detected at the nanoscopic level but has no functional effect on droplet formation at the macroscopic level, at all. The unusual behavior of $k_{macro,\ mercapto}$ is not found for k_{nano} which stabilizes around 0.80 after an initial decrease. In the nanoscopic approach, XPS reveals an amount of adsorbed polymer, which is averaged over a large surface area. In contrast, the contact angle is just defined by the edges of a water droplet, which corresponds to only a small local area. Therefore, inhomogeneities in the surface composition are strongly pronounced in k_{macro} , resulting in vast standard derivations, as seen for the mercapto-functionalized surface. Despite this inhomogeneity for mercapto-functionalized surfaces, k_{nano} proves the adsorption of considerable amounts of polymer even after long rinsing times. Consequently, the adhesiveness of HPC-PVP on a mercapto-functionalized surface can also be evaluated as strong. The cyano-functionalized surface cannot be addressed by XPS as overlapping signals arising from the coating and the polymer are not deconvoluted uniquely. Therefore, we refrained from a calculation of k_{nano}. However, the N 1s core level of the cyano groups on the surface is significantly attenuated with respect to the signal intensity before polymer incubation and, thus, indicates that a constant fraction of HPC-PVP remains adsorbed at the surface during all rinsing steps.

3.2.2. Protein-based polymer desorption

Analyzing the functionalized surfaces after a gliadin incubation by k_{macro} does not lead to meaningful values, e.g. $k_{macro}>3$ for amino-functionalized surfaces (compare Fig. 2 e). In contrast to the defined

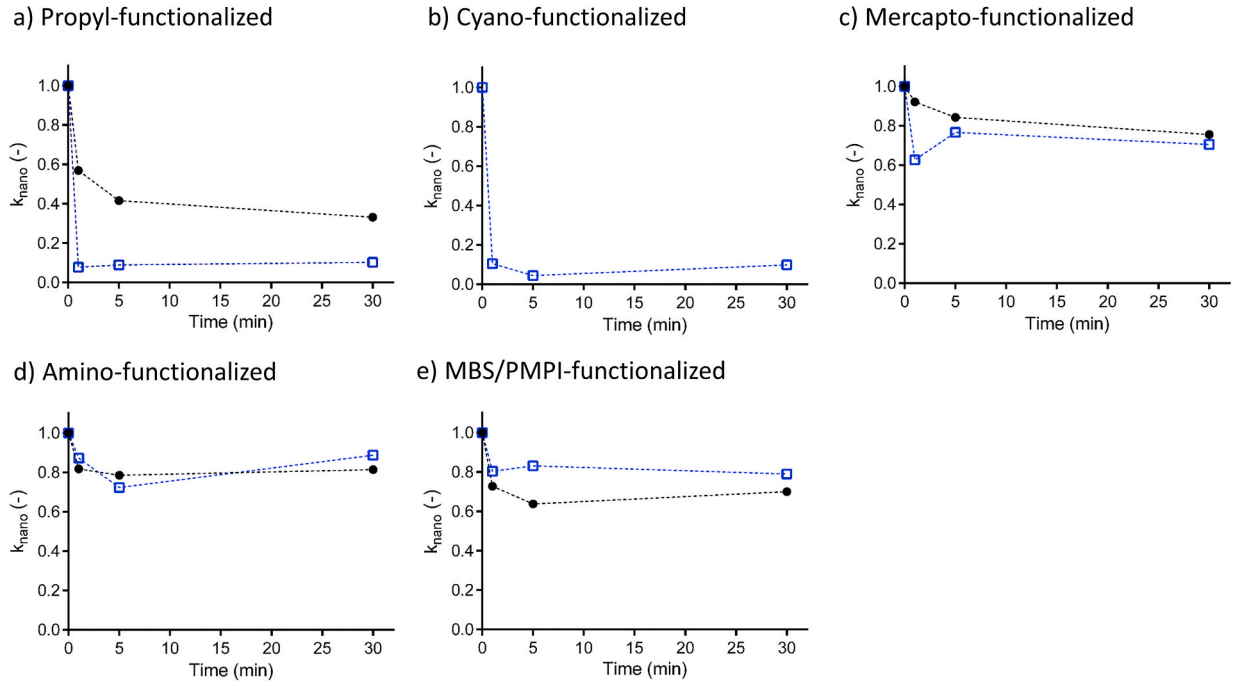

Fig. 3. Evaluation of polymer adhesiveness on functionalized SiO2 surfaces by XPS measurements. Adhesiveness, expressed by k_{nano}, over rinsing time for HPC-PVP (λ) and gliadin (o) in a) – e) depending on surface functionalization: Propyl-functionalized surface (a), cyano-functionalized surface (b), mercapto-functionalized surface (c), amino-functionalized surface (d) as well as MBS- (for gliadin) and PMPI (for HPC-PVP)-functionalized surface (e).

structure of the carbohydrate-based polymers, gliadin is a naturally occurring, large protein with a highly complex structure. In general, the high sensitivity of proteins easily leads to modified folding or denaturation. Changes in the protein structure might be induced due to the functional groups present at the coated surface during adsorption and explain the arbitrary results for k_{macro}. Nonetheless, k_{nano} provides reliable information about the adhesiveness of gliadin to different surface functionalizations. For propyl- and cyano-functionalized surfaces, k_{nano} significantly decreases after 1 min of rinsing to a negligible value of 0.03 and 0.10, respectively (see Fig. 3 a & b). In contrast, amino-, mercapto- and MBS-functionalized surfaces lead to a significantly lower decrease within the first minute of rinsing to values of 0.87, 0.62 and 0.85, respectively (see Fig. 3 c, d, e). Even longer rinsing times do not affect k_{nano}, anymore. Consequently, propyl- and cyano-functionalized surfaces offer a low adhesiveness for gliadin, whereas the adhesiveness to amino-, mercapto- and MBS-functionalized surfaces is significantly higher and corresponds to an increasing order of mercapto ~ amino < MBS. In general, all surface functionalizations show a decrease of k_{nano} after the first rinsing step, even if the adhesiveness is high. Based on the analyzed peak intensities, a desorption of weakly adsorbed multilayers of polymer can be concluded. After multilayer desorption, a stable monolayer remains at the surface, which appears as a stabilized value for both coefficients.

Depending on the polymer matrix (protein- or carbohydrate-based) and the surface functionalization, systems with different adhesivenesses in relation to each other were identified. Table 2 summarizes the functionalities of the different coatings. In combination with the observed desorption kinetics, possible interaction mechanisms with the polymers can be assumed. Cyano and propyl coatings enable weak and unspecific interactions, such as van der Waals forces, dipole-dipole, or hydrophobic interactions, explaining the fast polymer desorption during rinsing. Amino and mercapto coatings can induce more stable, specific and directed chemical interactions, like hydrogen or disulphide bonds. Mercapto-coated surfaces in combination with heterobifunctional cross-linkers enable strong specific covalent interactions.

3.3. Polymer adsorption controlled by functionalized glass beads

3.3.1. Validation of glass bead surface functionalization

A successful evaluation of the polymer adhesiveness using a flat model system paves the way towards the characterization of the impact of various particle surface functionalities on the network formation. Therefore, glass beads with a size range (2.60 μm–19.27 μm) typical for microscopic particles in foods, are coated with functionalized silanes. The presence of the desired functional groups at the glass bead surface is verified by fluorescence labeling in combination with CLSM imaging and by XPS measurements. In the first method, the binding of specific fluorescence dyes visualizes amino or mercapto groups. Fig. 4 shows a homogeneous dye layer across the z-axis of the glass bead surface proving a successful amino (a) and mercapto (b) coating. In contrast, for uncoated glass particles (Fig. 4 c) just a few undefined spots of fluorescence dye are visible which probably result from impurities [18] with a high affinity to the dye. Consequently, a successful coating can be concluded in case of amino and mercapto groups. Cyano and propyl coatings have low affinities to interact with dyes. Therefore, fluorescence labeling could not be performed. However, every functional group which was coated onto the glass bead surface could be detected by XPS. The characteristic photoemission lines already presented in chapter 3.1 are found for the glass beads, as well (see supplementary data).

3.3.2. Network formation depending on particle-polymer adhesiveness

To analyze the impact of the modified particle surface on the dynamic formation of protein- (gluten) or carbohydrate-based (HPC-PVP) polymerized matrices, a recording mixer (z-kneading system; Dough Lab) is used. With progressive network formation, the resistance against the induced deformation by the z-kneading geometry increases. This increasing resistance is recorded as mNm by the Dough Lab. Thus, plotting the recorded mNm against kneading time enables the monitoring of network formation (compare Fig. 5). Typical parameters to evaluate the network development are the peak resistance, which indicates the maximum network strength during the mixing process, and the development time to reach this peak. Comparing these two parameters for the different coatings and polymer matrices reveals a remarkable impact of the particle surface on the network development. As shown in Fig. 5, development time as well as peak resistance varies depending on the coating; the weakest network (lowest peak) is developed with the amino coating, followed by the propyl, cyano and mercapto coatings, whereas the systems with cross-linkers (MBS or PMPI) resulted in the strongest networks. Interestingly, this order of increasing peak resistance applies to both network types, protein- and carbohydrate-based. Comparing amino with propyl and cyano coatings, a lower or respectively unspecific adhesiveness towards the polymeric matrices exists in case of the latter ones. Assuming limited or nonspecific adsorption between the particle and the polymer allows unhindered polymerization of the network. This would result in higher peak resistance and thus, higher network strength. In contrast, the higher and more specific adhesiveness (hydrogen bonding) between amino coated particles and polymer might hinder the network formation due to the adsorption of polymers on the particles. However, this explanation does not apply to mercapto coated particles. For gluten proteins, thiol/disulphide exchange reactions are known to be essential regarding network formation. The addition of further thiol groups affects the network formation significantly [20–22]. Therefore, a divergent behavior of mercapto coated particles compared to other particles with similar adhesiveness (amino) is reasonable for gluten. Baudouin et al. (2020) suggested a mechanism of gluten network development depending on thiol interfering chemicals. In general, the thiol/disulphide exchanges are considered as determinant for the required mechanical energy since breaking of disulphide bonds leads to a release of mechanical stress. Blocking this reaction by introducing interfering chemicals like *N*-ethylmaleimide (NEM), which binds to free SH groups, leads to an increase of mechanical stress. Since energy dissipation by

Table 2
Resulting interactions with the polymer matrix depending on surface functionalization.

Functional group of coating		Supposed mediated interaction with the matrix type:	
Type	**Properties**	**Protein (gliadin)**	**Carbohydrate (HPC-PVP)**
Cyano	Strongly dipolar, hydrophilic, prevents chemical binding of proteins [19]	Weak, unspecific (Van der Waals forces, dipole-dipole)	Strong, unspecific (dipole-dipole)
Propyl	Non-polar, hydrophobic	Weak, unspecific (hydrophobic interactions, Van der Waals forces)	Weak, unspecific (Van der Waals forces)
Amino	Polar, hydrophilic	Intermediate strong, specific (H-bonds)	Strong, specific (H-bonds)
Mercapto	Polar, hydrophilic	Intermediate strong, specific (H-bonds, disulfide bonds)	Strong, specific (H-Bonds)
MBS	Covalent cross-linking	Strong, highly specific (covalent binding with primary amines)	Not used
PMPI	Covalent cross-linking	Not used	Intermediate strong, highly specific (covalent binding with hydroxyl groups)

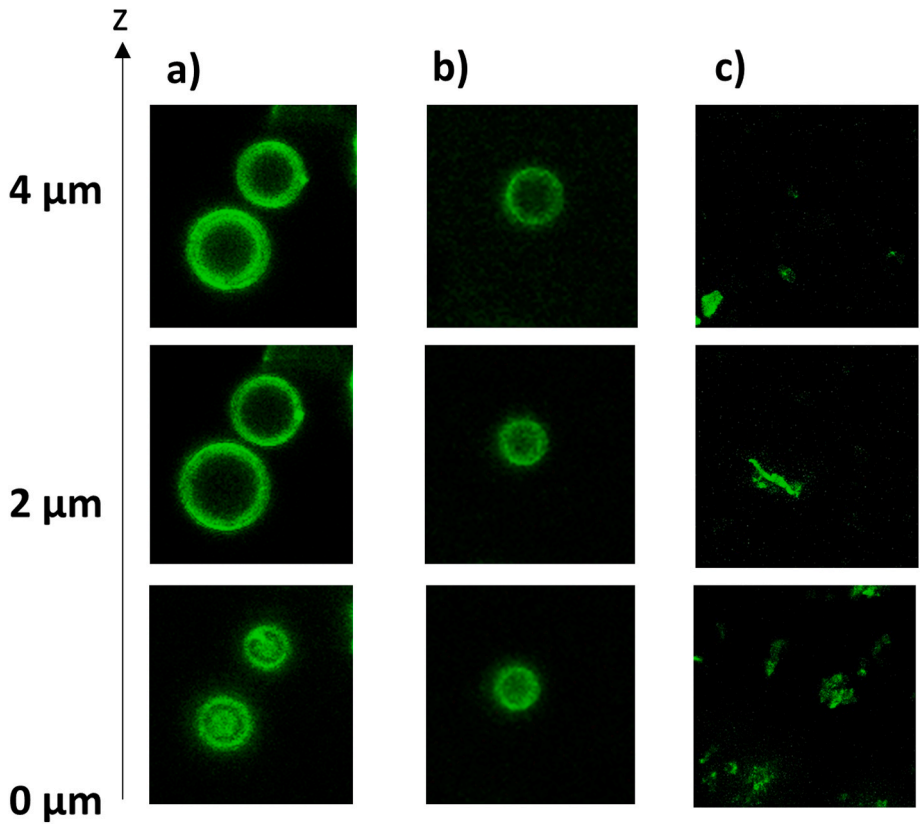

Fig. 4. Validation of glass bead functionalization by CLSM imaging: Glass beads at three different z-axis positions. a) amino-coated glass beads labeled with fluorescein-5-isothiocyanate. b) mercapto-coated glass beads labeled with fluorescein-5-maleimide. c) uncoated glass beads with fluorescein-5-isothiocyanate.

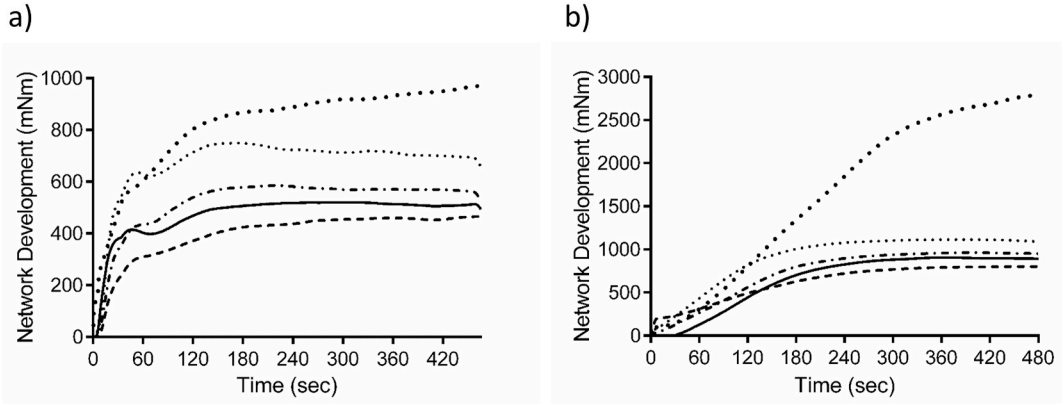

Fig. 5. Network formation monitored by a recording mixer a) for gluten mixtures and b) for HPC-PVP glass bead mixtures with varying coatings: mercapto (· · ·), amino (- - -), propyl (—), cyano (· - · -) as well as MBS for gluten in a) and PMPI for HPC-PVP in b) (· · ·).

breaking disulphide bonds is not possible anymore, a direct stress transfer along the polymer chain is assumed [21]. Adding mercapto coated particles shows effects similar to thiol interfering chemicals. The additional thiol groups on the particle surface can also influence the thiol/disulphide exchanges of gluten by blocking free thiol groups. As described by Baudouin et al. (2020) the resulting direct stress transfer to the polymeric matrix causes the higher mNms and a shortened network development time. However, this approach cannot explain the high peak resistance of mercapto coated particles in carbohydrate-based systems. The molecular mechanisms causing the high peak resistance remain concealed. The addition of particles which are supposed to covalently interact with the polymers (MBS or PMPI coated) causes significant effects. For protein-based systems, the peak resistance is almost twice as high and the development time two to three times longer than for all other coatings; the peak resistance and development time in the carbohydrate-based system is even outside the detection limit. On the one hand, the strong adhesiveness between particles and polymers provides a very effective stress transfer [23], which results in high mNm for MBS- or PMPI-coated particles. On the other hand, the polymeric linking is hindered/delayed and results in long development times. Regarding the adhesiveness of coatings, the protein-based networks are affected stronger by the different coating types than the carbohydrate-based systems. The development time of gluten-based systems range from 3.2 min for mercapto-coated particles to 6.0 min for amino-coated particles. In contrast, the HPC-PVP-based systems just range from a development time of 6.1 min for propyl to 6.7 min for

mercapto. As already mentioned, the adhesiveness between particle and polymers can hinder the network development by an adsorption, induced by the adhesiveness, and a desorption, induced by the mechanical forces, until a stable equilibrium of adsorbed particles and inter-polymeric junctions exists. Depending on the adhesiveness and the type of particle-polymer interaction, the network development time varies. Since gluten has a vast variety of polymeric junction types (hydrophobic and van der Waals interactions, H-bonds, disulfide-bonds, entanglements), each of the particle coatings will affect a different type of network junction, resulting in very different network development times. In contrast to the gluten polymer, the network structure of HPC-PVP is mainly based on hydrogen-bonds and only to a minor amount on entanglements and polar forces [24]. Consequently, each coating type affects the same network junction type (for hydrogen bonding). The similar adsorption mechanisms of the particles, independent of their coating, could explain the small range of network development times for the HPC-PVP matrix.

4. Conclusion

Within the scope of this study, the impact of particle surface functionality on the network formation in food-based matrices was analyzed. By using a model system, the adhesiveness of protein- and carbohydrate-based polymers was evaluated on defined surfaces, functionalized by different coatings, respectively. The combination of macro- and nanoscopic analytics enables to determine the degree of interaction between polymer and coating. As a result, systems with an adhesiveness ranging from weak unspecific adsorption to strong specific adsorption of polymers were established and can be used to imitate naturally occurring interactions in particle-polymer-based food systems. Based on the findings about polymer adhesiveness with a specific coating, the impact of particle surface functionality on network development could be analyzed in a new way. Independent of food matrix type, particle adhesiveness influences the mixing time for reaching maximum network strength, thus indicating the ability of particle surface functionality in affecting network formation. In particular, the heterogeneity of network junction types seems to enhance the effect of particle surface functionalities on the network development. Polymeric networks, mainly formed by one junction type (HPC-PVP), exhibit a smaller range in network development time as heterogenic networks, consisting of many different junctions (gluten). The observations made in studies, which analyze the impact of network modifying chemicals (e.g. urea or NEM) on network development, are in accordance with the observed modifications of network development by using coated particles. For example, mercapto coated particles lead to a shorter network development time and a more effective stress transfer in a similar way as thiol interfering chemicals cause. At the one hand, this can be considered as a proof of principle for using silane coated particles to control the adhesion/interactions between particles and polymers, since the blocking of polymeric functional groups by particles resulted in the same mechanical trends as adding the pure chemicals. On the other hand, this implies that the presented approach offers a powerful method for analyzing the impact of particle-polymer interfaces in food based systems. The large number of commercial available silanes enables the imitation of nearly every natural occurring surface in a very defined and reproducible way. Combining the presented approach with fundamental rheological tests, contributes to a deeper understanding of particle-polymer interactions on the overall mechanical properties in food and is considered as following step.

CRediT authorship contribution statement

Silvia Brandner: Conceptualization, Methodology, Writing – original draft. **Tim Kratky:** Investigation, Formal analysis, Writing – review & editing. **Kerstin Holtz:** Investigation, Validation. **Thomas Becker:** Supervision. **Mario Jekle:** Writing – review & editing.

Declaration of competing interest

The authors declare that they have no known competing financial interests or personal relationships that could have appeared to influence the work reported in this paper.

Acknowledgements

This research did not receive any specific grant from funding agencies in the public, commercial, or not-for-profit sectors.

Appendix A. Supplementary data

Supplementary data to this article can be found online at https://doi.org/10.1016/j.compscitech.2021.108864.

References

[1] L. Bokobza, O. Rapoport, Reinforcement of natural rubber, J. Appl. Polym. Sci. 85 (11) (2002) 2301–2316, https://doi.org/10.1002/app.10858.
[2] D.C. Edwards, Polymer-filler interactions in rubber reinforcement, J. Mater. Sci. 25 (10) (1990) 4175–4185, https://doi.org/10.1007/BF00581070.
[3] W. Wijaya, A.R. Patel, A.D. Setiowati, P. van der Meeren, Functional colloids from proteins and polysaccharides for food applications, Trends Food Sci. Technol. 68 (2017) 56–69, https://doi.org/10.1016/j.tifs.2017.08.003.
[4] C.C. Maningat, P.A. Seib, S.D. Bassi, K.S. Woo, G.D. Lasater, Chapter 10 - wheat starch: production, properties, modification and uses, in: James BeMiller, Roy Whistler (Eds.), Starch, third ed., Academic Press, San Diego, 2009, pp. 441–510.
[5] Y. Li, K.T. Ramesh, Influence of particle volume fraction, shape, and aspect ratio on the behavior of particle-reinforced metal–matrix composites at high rates of strain, Acta Mater. 46 (16) (1998) 5633–5646, https://doi.org/10.1016/S1359-6454(98)00250-X.
[6] Q.W. Yuan, J.E. Mark, Reinforcement of poly(dimethylsiloxane) networks by blended and in-situgenerated silica fillers having various sizes, size distributions, and modified surfaces, Macromol. Chem. Phys. 200 (1) (1999) 206–220, https://doi.org/10.1002/(SICI)1521-3935(19990101)200:1<206:AID-MACP206>3.0.CO;2-S.
[7] J. Fröhlich, W. Niedermeier, H.-D. Luginsland, The effect of filler–filler and filler–elastomer interaction on rubber reinforcement, Compos. Appl. Sci. Manuf. 36 (4) (2005) 449–460, https://doi.org/10.1016/j.compositesa.2004.10.004.
[8] D. Zhang, T. Mu, H. Sun, Effects of starch from five different botanical sources on the fermentation and gelatinization properties of starch–gluten model doughs, Starch - Stärke 71 (1–2) (2019) 1800034, https://doi.org/10.1002/star.201800034.
[9] A. Pauly, B. Pareyt, M.A. Lambrecht, E. Fierens, J.A. Delcour, Impact of puroindolines on semisweet biscuit quality: a fractionation–reconstitution approach, Cereal Chem. 90 (6) (2013) 564–571, https://doi.org/10.1094/CCHEM-04-13-0075-R.
[10] A. Graßberger, P. Schieberle, P. Koehler, Fractionation and reconstitution of wheat flour – effect on dough rheology and baking, Eur. Food Res. Technol. 216 (3) (2003) 204–211, https://doi.org/10.1007/s00217-002-0645-4.
[11] J. Rouillé, G. Della Valle, J. Lefebvre, E. Sliwinski, T. vanVliet, Shear and extensional properties of bread doughs affected by their minor components, J. Cereal. Sci. 42 (1) (2005) 45–57, https://doi.org/10.1016/j.jcs.2004.12.008.
[12] P.M. Baldwin, C.D. Melia, M.C. Davies, The surface chemistry of starch granules studied by time-of-flight secondary ion mass spectrometry, J. Cereal. Sci. 26 (3) (1997) 329–346, https://doi.org/10.1006/jcrs.1997.0132.
[13] S.M. Finnie, R. Jeannotte, C.F. Morris, M.J. Giroux, J.M. Faubion, Variation in polar lipids located on the surface of wheat starch, J. Cereal. Sci. 51 (1) (2010) 73–80, https://doi.org/10.1016/j.jcs.2009.09.007.
[14] H.R.C. Petrofsky Ke, Rheological properties of dough made with starch and gluten from several cereal sources, Cereal Chem. 72 (1) (1995) 53–58.
[15] P. Fustier, F. Castaigne, S.L. Turgeon, C.G. Biliaderis, Semi-sweet biscuit making potential of soft wheat flour patent, middle-cut and clear mill streams made with native and reconstituted flours, J. Cereal. Sci. 46 (2) (2007) 119–131, https://doi.org/10.1016/j.jcs.2006.10.011.
[16] K.J. Ryan, M.S. Brewer, Model system analysis of wheat starch-soy protein interaction kinetics using polystyrene microspheres, Food Chem. 92 (2) (2005) 325–335, https://doi.org/10.1016/j.foodchem.2004.08.005.
[17] N.M. Edwards, J.E. Dexter, M.G. Scanlon, Starch participation in durum dough linear viscoelastic properties, Cereal Chem. 79 (6) (2002) 850–856, https://doi.org/10.1094/CCHEM.2002.79.6.850.
[18] Silvia Brandner, Thomas Becker, Mario Jekle, Wheat dough imitating artificial dough system based on hydrocolloids and glass beads, J. Food Eng. 223 (2018) 144–151, https://doi.org/10.1016/j.jfoodeng.2017.12.014.
[19] J.R. Wayment, J.M. Harris, Controlling binding site densities on glass surfaces, Anal. Chem. 78 (22) (2006) 7841–7849, https://doi.org/10.1021/ac061392g.
[20] Amogh Ambardekar, Modifications in Visco-Elasticity of Gluten by Diacetyl Tartaric Acid Ester of Monoglyceride (DATEM), Ascorbic Acid, Urea and

Dithiothreitol and its Effects on Mixing and Baking Properties in Commercial Wheat Flours, Dissertation, 2009.

[21] F. Baudouin, T.L. Nogueira, A. van der Mijnsbrugge, S. Frederix, A. Redl, M.-H. Morel, Mechanochemical activation of gluten network development during dough mixing, J. Food Eng. 283 (2020) 110035, https://doi.org/10.1016/j.jfoodeng.2020.110035.

[22] P. Chen, R. Li, R. Zhou, G. He, P. Shewry, Heterologous expression and dough mixing studies of a novel cysteine-rich avenin-like protein, Cereal Res. Commun. 38 (3) (2010) 406–418, https://doi.org/10.1556/CRC.38.2010.3.11.

[23] S.-Y. Fu, X.-Q. Feng, B. Lauke, Y.-W. Mai, Effects of particle size, particle/matrix interface adhesion and particle loading on mechanical properties of particulate–polymer composites, Compos. B Eng. 39 (6) (2008) 933–961, https://doi.org/10.1016/j.compositesb.2008.01.002.

[24] L.I. Kutsenko, Y.G. Santuryan, E.B. Karetnikova, I.V. Gofman, A.M. Bochek, E. F. Panarin, Properties of the methyl cellulose-polyvinylpyrrolidone binary system in solution and in the solid state, Russ. J. Appl. Chem. 80 (5) (2007) 771–776, https://doi.org/10.1134/S1070427207050163.

[25] Jill Chastain, Roger C. King Jr., Handbook of X-Ray Photoelectron Spectroscopy, 40th ed., Perkin-Elmer Corporation, 1992.